Dielectric properties and charge transport in the $(Sr,La)NbO_{3.5-x}$ system

V. Bobnar,* P. Lunkenheimer, J. Hemberger, and A. Loidl
Experimentalphysik V, Elektronische Korrelationen und Magnetismus, Institut für Physik, Universität Augsburg, D-86135 Augsburg, Germany

F. Lichtenberg and J. Mannhart
Experimentalphysik VI, Elektronische Korrelationen und Magnetismus, Institut für Physik, Universität Augsburg, D-86135 Augsburg, Germany

(Received 4 April 2001; revised manuscript received 26 November 2001; published 4 April 2002)

The dielectric response of layered perovskite-related insulating $SrNbO_{3.5}$ and conducting $SrNbO_{3.41}$, $SrNbO_{3.45}$, and $La_{0.2}Sr_{0.8}NbO_{3.5}$ single crystals is investigated. The measurements are performed along the *c* axis, i.e., perpendicular to the layers, in the frequency range from 1 MHz to 1.8 GHz. The intrinsic dielectric properties could be monitored only at such relatively high measuring frequencies, since strong contact contributions at the sample-electrode interface dominate at low frequencies. In addition to the known phase transitions in the $SrNbO_{3.5}$ compound, a phase transition at $T \approx 300$ K in $SrNbO_{3.41}$ and $SrNbO_{3.45}$ is reported here. The frequency-dependent ac conductivity in all three conducting compounds follows the universal dielectric response behavior. Together with results on the dc conductivity, this finding indicates that hopping of localized charge carriers, most likely of polaronic character, is the dominating charge-transport process. For all $SrNbO_{3.5-x}$ compounds, relatively high values of the dielectric constant are found.

DOI: 10.1103/PhysRevB.65.155115 PACS number(s): 72.20.Fr, 77.22.Ch, 77.84.Dy

I. INTRODUCTION

For a long time transition-metal oxides have been the focus of solid-state research. Strong electronic correlations of the partly filled *d* bands in addition to cooperative phenomena of internal degrees of freedom, such as spin, charge, orbital moments, and lattice degrees of freedom, are responsible for an enormous variety of possible ground states: ferroelectricity with high transition temperatures, metallic and insulating ferromagnetism including colossal magnetoresistance effects in perovskite manganites, high-temperature superconductivity in layered copper oxides, unconventional (*d*- or *p*-wave pairing) superconductivity in Sr_2RuO_4, low-dimensional magnetism, and low-dimensional metallic behavior are attracting continuing and considerable attention.[1] Many of the systems are close to a correlation-induced metal-to-insulator transition, and close to the transition many interesting cooperative phenomena show up.[1]

A series of transition-metal oxides, $SrNbO_{3.5-x}$, was synthesized and studied a decade ago,[2] and recently in more detail.[3] These orthorhombic compounds belong to a series of $A_nB_nO_{3n+2}$, and are derived from the three-dimensional network of the ABO_3 perovskite structure by separating the BO_6 octahedra parallel to the (110) planes, and introducing additional oxygen. In accordance with Refs. 2 and 3, we define crystallographic axes such that the *a* axis is the direction where the NbO_6 octahedra are chainlike connected, and the *c* axis is the longest axis perpendicular to the layers. They exhibit very different properties depending on the oxygen content. $SrNbO_{3.5}$ ($x=0$, $n=4$) is a ferroelectric with an enormously high transition temperature, and was already intensively studied using different experimental techniques, including high-resolution electron microscopy,[4] Raman scattering,[5] elastic,[6] and dielectric-spectroscopy studies.[7–10] The latter revealed that the system undergoes a ferroelectric transition at 1615 K, with the polarization along the *b* axis.[8] At 488 K a ferroelectric-to-incommensurate phase transition occurs,[9] and finally a transition into another ferroelectric state, which is polarized in the *bc* plane, takes place.[10] Transition temperatures of 100 (Ref. 10) and 117 K (Ref. 7) was reported for the second ferroelectric phase transition. Due to its high coercive field and high thermal stability, $SrNbO_{3.5}$ offers a great possibility for utilization as a material for nonvolatile ferroelectric memories. For this application it was prepared as a single-phase thin film, processed at a very low temperature of 600 °C.[11]

With decreasing oxygen content the insulating compound with $x=0$ ($n=4$) becomes a layered electronic conductor with $x \approx 0.1$ ($n=5$). Between these two oxygen contents a further compound appears for $x \approx 0.05$ ($n=4.5$) which involves a well-ordered stacking sequence of $n=4$ and 5 subunits. The structure type *n* is only determined by the oxygen content. Another way of tuning the electronic properties of this system is a partial substitution of divalent strontium by trivalent lanthanum. Similar to the decrease of the oxygen content, this procedure also results in electron doping, leaving niobium in a mixed-valent state (Nb^{5+}/Nb^{4+}).[2,3]

Several studies of these strongly anisotropic compounds were already reported. They focused mainly on structural, magnetic, and electronic properties, using magnetic susceptibility measurements,[2,3,12] near-edge x-ray-absorption spectroscopy,[13,14] angle-resolved photoemission,[13–16] dc resistivity measurements,[2,3,16] optical spectroscopy,[16] and, very recently, NMR and EPR measurements.[12] It was found that conducting $(Sr,La)NbO_{3.5-x}$ compounds exhibit quasi-one-dimensional metallic conductivity along the *a* axis at elevated temperatures, whereas at lower temperatures a metal-semiconductor transition appears.[3,13–16] Along the *b* and *c* axes only a semiconducting behavior was observed.[3,16] In addition, in the case of the semiconducting behavior, ther-

mally activated electrical transport was reported in parts of the temperature range.[2,3,16] On the other hand, dielectric studies of these compounds have not yet been reported.

We performed detailed dielectric investigations of $SrNbO_{3.41}$, $SrNbO_{3.45}$, $SrNbO_{3.5}$, and $La_{0.2}Sr_{0.8}NbO_{3.5}$ single crystals along the *c* axis in a frequency range from 1 MHz to 1.8 GHz. We show that, due to high contact contributions, the intrinsic dielectric response can be determined only by performing measurements at such high frequencies.

The experimental procedures are summarized in Sec. II. The results and analysis of measurements of all four compounds are given in Sec. III. While all the transitions observed in the $SrNbO_{3.5}$ compound were already reported in the literature, we have detected new transitions in the other two $SrNbO_{3.5-x}$ compounds. A discussion of the results is given in Sec. IV. From the results of both dc and ac measurements, we conclude that hopping of localized charge carriers, rather than a thermally activated behavior, governs the electrical transport along the *c* axis in the $(Sr,La)NbO_{3.5-x}$ system. From an analysis of the detected universal dielectric response (UDR) behavior and the relatively high values of the high-frequency dielectric constant, a polaronic nature of the charge carriers seems most likely. Finally, the results are summarized in Sec. V.

II. EXPERIMENTAL PROCEDURES

$SrNbO_{3.5}$, $SrNbO_{3.45}$, $SrNbO_{3.41}$, and $La_{0.2}Sr_{0.8}NbO_{3.5}$ single crystals were grown by the floating-zone melting technique, as described in Refs. 2 and 3. The oxygen content of the samples was determined thermogravimetrically with an accuracy of $\approx 0.3\%$.[3] The typical thickness of the samples was 0.2 mm. In order to perform dielectric measurements in the radio-frequency range, the sample was mounted at the end of a coaxial air line, connecting the inner and outer conductors.[17] The complex reflection coefficient Γ was recorded in a frequency range from 1 MHz to 1.8 GHz using a HP4291 impedance analyzer. The complex dielectric constant or complex conductivity can be calculated from Γ after proper calibration using three standard samples, thus eliminating the influences of the coaxial line and sample holder. The end of the coaxial line was either brought into a nitrogen-gas heated/cooled cryostat, where the dielectric response was measured in the temperature range of 120–550 K, or brought into a ^{4}He cryostat, which enables measurements in the temperature range of 1.5–300 K. Thus by combining both methods we were able to determine the dielectric response in the temperature range of 1.5–550 K. In all cases the dielectric response was monitored during temperature scans with a typical rate of ± 0.5 K/min.

The reflectometric measurement technique requires a two-point contact configuration, which implies that contacts also contribute to the measured response. We used two different types of electrodes—the surface area of the samples, typically having dimensions of 3×2 mm^2, was covered either by gold electrodes, applied using the sputtering technique ($SrNbO_{3.45}$, $SrNbO_{3.5}$, and $La_{0.2}Sr_{0.8}NbO_{3.5}$), or by silver paint electrodes ($SrNbO_{3.41}$). Silver paint electrodes have the advantage that they can be easily removed after the measurement, which allows a further investigation of the same sample in different directions or using different electrodes. All measurements reported in this work were performed with the electrical field directed parallel to the *c* axis, thus determining the dielectric response perpendicular to the layers.

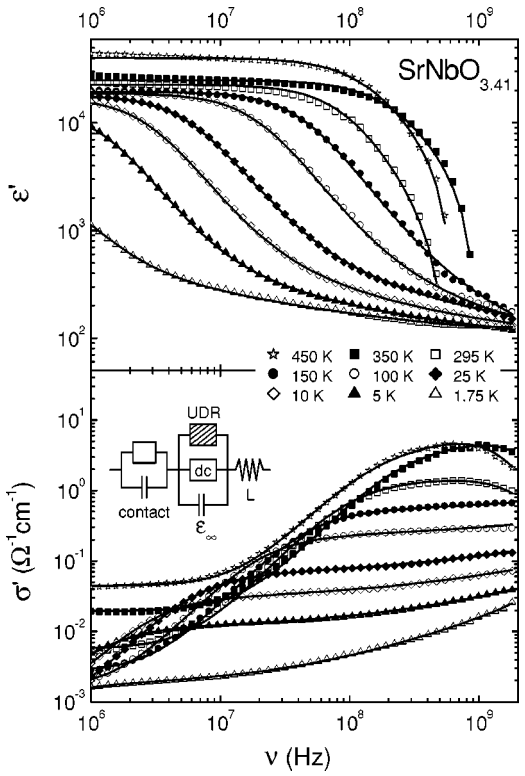

FIG. 1. Frequency dependence of the dielectric constant ε' and conductivity σ' measured at several temperatures in a $SrNbO_{3.41}$ single crystal. Solid lines through the experimental data are fits using the equivalent circuit, which is also indicated in the figure.

III. RESULTS AND ANALYSIS

This section gives a description of the dielectric results and their analysis measured as a function of frequency in a range from 1 MHz to 1.8 GHz, and of temperature in the range of 1.5–550 K in $SrNbO_{3.41}$, $SrNbO_{3.45}$, $SrNbO_{3.5}$, and $La_{0.2}Sr_{0.8}NbO_{3.5}$ single crystals.

A. Dielectric properties of $SrNbO_{3.41}$ single crystal

Figure 1 shows the frequency dependence of the dielectric constant ε' and conductivity σ' measured at several temperatures in $SrNbO_{3.41}$. A distinctive downward step in ε', which is accompanied by a steplike increase in σ' and a corresponding peak in the dielectric loss $\varepsilon'' \sim \sigma'/\omega$ (not shown), can be observed at higher temperatures. Such a feature often indicates a relaxation process of dipolar degrees of freedom. However, in the present case some observations strongly favor the contact contribution as the origin of this behavior: At first, for low frequencies, ε' approaches unreasonably high values of the order of 10^4. In addition, the steps in ε' and the corresponding peaks in ε'' have relatively small

widths, following the single-exponential Debye response,[18,19] which is only rarely realized for dipolar relaxation.

The reason for such strong contact contributions presumably is the formation of Schottky diodes at the interface of metal electrodes and semiconductor, which leads to a thin surface layer of low carrier concentration. It could also be caused by deviations from stoichiometry (e.g., deviations in the oxygen content) or the accumulation of defect states at the surface of the sample, leading to a thin, insulating layer. Contact contributions are usually modeled by a parallel *RC* circuit, which is connected in series to the sample.[18–20] At high frequencies the contact capacitance *C* is effectively shorted, thus allowing the observation of the intrinsic response of the material. The time constant of the circuit increases with decreasing temperature due to the semiconducting character of the resistance. Therefore, both steps in ε' and σ' shift to lower frequencies, and the intrinsic response can be detected down to lower frequencies when decreasing the temperature. Within this framework, the high values of ε' at low frequencies can be understood by taking into account that, at low frequencies, the response is dominated by the thin contact region.

Focusing now on the intrinsic contribution, Fig. 1 shows that, after contact, step σ' reaches a plateau, which can be identified with the dc conductivity σ_{dc}, while at higher frequencies the values continuously increase (this is best demonstrated at temperatures of 25, 10, and 5 K). Concomitantly, following the contact step, ε' approaches a shallow power-law decrease. The frequency dependence of the intrinsic conductivity can be thus well described by the so-called universal dielectric response, with the addition of a dc conductivity:[18]

$$\sigma' = \sigma_{dc} + \sigma_0 \omega^s, \tag{1}$$

$$\sigma'' = \omega \varepsilon_0 \varepsilon' = \tan(s\pi/2)\sigma_0 \omega^s, \tag{2}$$

with ε_0 being the permittivity of free space and $s<1$. There are several theoretical approaches deducing such behavior from the microscopic transport properties, including hopping over or tunneling of the charge carriers through an energy barrier separating different localized states.[21,22]

Therefore, in order to analyze the measured data we have used the equivalent circuit, presented in Fig. 1. A parallel *RC* circuit, describing the contact contribution, is connected in series to the sample, whose intrinsic response is described by the dc conductivity, the universal dielectric response, and ε_∞, the latter taking account of the ionic and electronic polarizabilities of the sample. It can be seen in Fig. 1 that, especially at high temperatures, the measured values of both ε' and σ' start to decrease at high frequencies. At the highest frequencies, ε' even becomes negative. This can be ascribed to the inductance *L* of the system. Therefore, an inductance connected in series with the sample and contact is included in the equivalent circuit. Solid lines through the experimental data in Fig. 1 are fits using this equivalent circuit, performed simultaneously for ε' and σ'. The agreement is very good; thus the equivalent circuit gives a good description of the measured dielectric response.

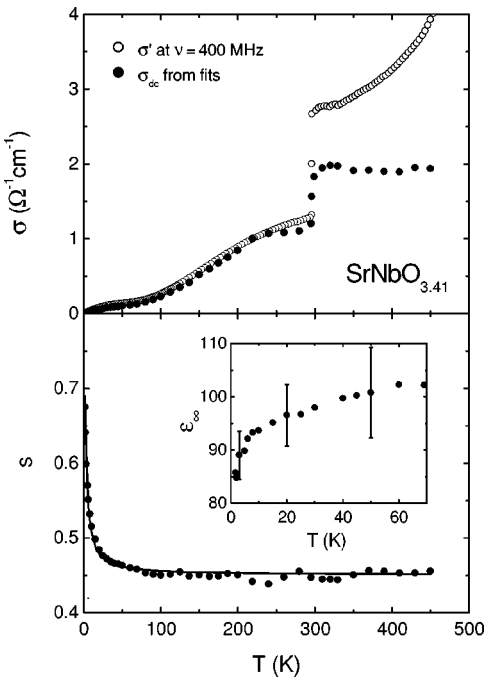

FIG. 2. Temperature dependence of σ_{dc}, ε_∞, and *s*, determined from the fits presented in Fig. 1. In addition, experimental data of σ', measured at 400 MHz, are shown. The solid line through the $s(T)$ data is a fit with a model for small polaron tunneling (Refs. 18–20).

Figure 2 shows the temperature dependence of the fit parameters σ_{dc}, ε_∞, and *s*, which describe the intrinsic properties of $SrNbO_{3.41}$. σ_{dc} shows a strong increase at $T \approx 300$ K, indicating a phase transition occurring at this temperature. From the present data we cannot deduce the nature of this transition, however, we suspect that it might be a structural one. This transition can also be seen in the raw data: the data of σ' measured at frequency of 400 MHz are also presented in Fig. 2. While at lower temperatures σ' (400 MHz) almost coincides with σ_{dc} obtained from the fits, at higher temperatures it tends to differ from σ_{dc}, mainly due to the inductance contributions. On the other hand, σ', measured at much lower frequencies, strongly differs from the data, obtained from the fits, due to the contact contribution. In Sec. IV we will discuss the possible mechanisms governing the electrical transport in the $SrNbO_{3.41}$ system.

The temperature dependence of the UDR exponent *s* is almost independent of temperature above 100 K, but it starts to increase rapidly when lowering the temperature below 100 K. Such a dependence was predicted for the tunneling of small polarons[21–23] (originally this model was developed for overlapping large polarons,[21,22] but in Ref. 23 it was argued that in fact it is applicable to small polarons). Indeed, the solid line through the experimental data represents a good fit using this model, though with a very low value of the hopping barrier $W_\infty = 1.5$ meV. One has to be aware that the small polaron tunneling model also predicts a frequency dependence of *s*. Therefore, Eqs. (1) and (2) should no longer be valid in a strong sense, i.e. with $s = \text{const}$. However, the present data reveal a "pure" ν^s contribution only in rela-

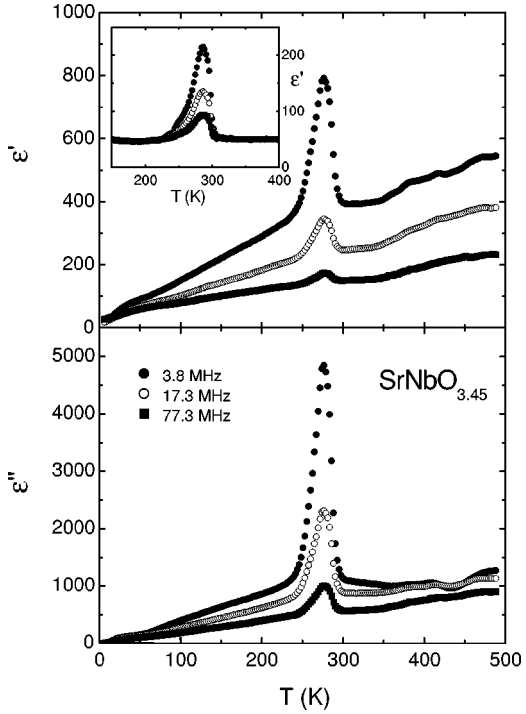

FIG. 3. Temperature dependence of the real (ε') and imaginary (ε'') parts of the complex dielectric constant measured at several frequencies in a $SrNbO_{3.45}$ single crystal. The inset shows the temperature-dependent ε' data in another $SrNbO_{3.45}$ crystal with lower ac conductivity, which is probably the result of a slightly different oxygen content. Here the value of $\varepsilon_\infty \approx 50$ was determined.

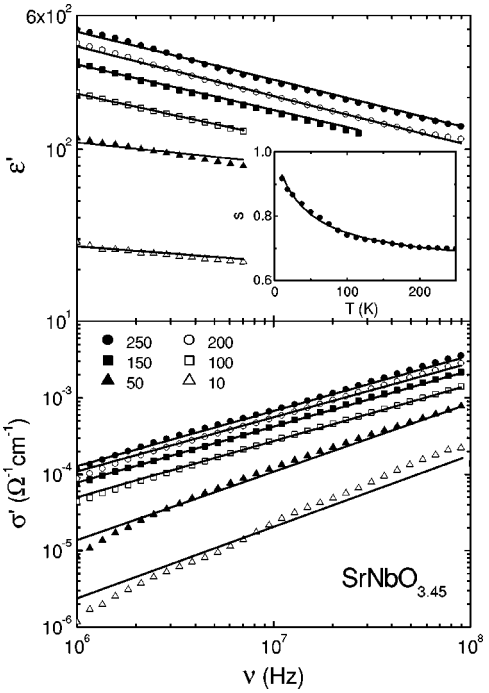

FIG. 4. Frequency dependence of the dielectric constant ε' and conductivity σ' measured at several temperatures in a $SrNbO_{3.45}$ single crystal. Solid lines through the experimental data are fits to the UDR. The inset shows the temperature dependence of the exponent *s*, with the solid line being a fit with a model for small polaron tunneling.

tively small frequency ranges and it can be assumed that the rather weak $\ln(\nu)$ dependence predicted for $s(\nu)$ (Refs. 21 and 22) leads only to small deviations from Eqs. (1) and (2). For the fit of $s(T)$ shown in Fig. 2, a frequency of 1 GHz was assumed. Values of the other two fitting parameters are $\tau_0 = 1.1 \times 10^{-13}$ s and $\alpha r_0 = 3.5$, where τ_0 is an inverse attempt frequency and αr_0 is the reduced polaron radius.[21,22]

Finally, values of ε_∞, presented in Fig. 2, are almost independent of temperature below 70 K. The inductance contribution, which dominates at higher frequencies, also prevents us from determining values of ε_∞ at higher temperatures. In any case, it can be seen clearly that the intrinsic values of ε are much smaller than one could conclude if the dielectric response would be measured at frequencies below 1 MHz only.

B. Dielectric properties of $SrNbO_{3.45}$ single crystal

The temperature dependence of the real and imaginary part of the complex dielectric constant, measured at several frequencies in $SrNbO_{3.45}$, is shown in Fig. 3. At $T \approx 280$ K a phase transition occurs, which is reflected in a strong anomaly in both ε' and ε''. The high conductivity of the samples prevented us from measuring the polarization hysteresis loop at temperatures either above or below the transition temperature to check if this is a polar phase transition. Nevertheless it may be suspected that this transition is connected with transitions which take place in the $SrNbO_{3.5}$ system, and will be described in Sec. IV C.

Figure 4 shows the frequency dependence of the dielectric constant ε' and conductivity σ' measured at several temperatures. Due to problems with calibration at higher frequencies, the usable frequency range in this measurement is restricted to $\nu < 100$ MHz. In contrast to the results in the $SrNbO_{3.41}$ sample, no dc plateau and also no contact contribution is observed in the measured σ' data. The absence of contact contributions in this sample may indicate that no Schottky diodes are formed, probably due to the use of gold electrodes (instead of silver for $SrNbO_{3.41}$) or due to the lower charge-carrier concentration leading to a different band configuration at the interface. The experimental data can be described by using only the UDR. The temperature dependence of the parameter *s* is shown in the inset to Fig. 4, and can be again described by the model for small polaron tunneling, yielding values of $W_\infty = 54$ meV, $\tau_0 = 2.5 \times 10^{-15}$ s, and $\alpha r_0 = 6.5$. The resulting value of the hopping barrier is thus higher in $SrNbO_{3.45}$ than in $SrNbO_{3.41}$. Together with the decreased number of charge carriers, this leads to the observed lower conductivity of $SrNbO_{3.45}$.

Partly due to the somewhat restricted frequency range, the frequency dependence of ε', as shown in Fig. 4, does not saturate at higher frequencies, which prevented the determination of ε_∞ in this particular sample. However, the inset to Fig. 3 shows the temperature-dependent ε' data measured in another $SrNbO_{3.45}$ sample. In this sample values of both ε' and ε'' are almost independent of frequency at temperatures above and below the phase transition. Obviously this occurs due to the lower ac conductivity of this sample, which might

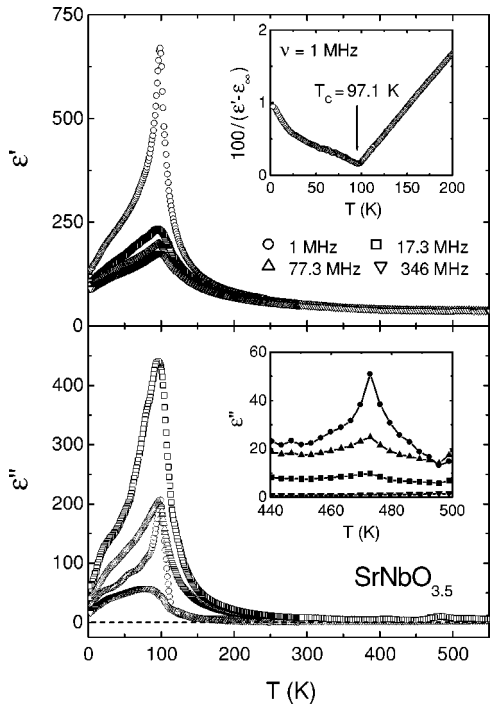

FIG. 5. Temperature dependence of the real (ε') and imaginary (ε'') parts of the complex dielectric constant measured at several frequencies in a $SrNbO_{3.5}$ single crystal. The upper inset shows the inverse of the real part of the dielectric constant after subtraction of the background in the temperature region around the ferroelectric phase transition. The lower inset shows the ε'' data measured at frequencies of 3.8 MHz, 346 MHz, 732 MHz, and 1.8 GHz (from top to bottom) in the temperature region around the ferroelectric-to-incommensurate phase transition.

be the result of a slightly different oxygen content. In this sample one can directly determine the value of $\varepsilon_\infty \approx 50$, which strongly differs from the $SrNbO_{3.41}$ system, where the corresponding value was $\varepsilon_\infty \approx 95$ (cf. Fig. 2).

C. Dielectric properties of $SrNbO_{3.5}$ single crystal

Figure 5 shows the temperature dependence of the real and imaginary parts of the complex dielectric constant measured at several frequencies in $SrNbO_{3.5}$. A strong anomaly is observed at $T \approx 100$ K, corresponding to the ferroelectric transition already reported in Ref. 10. The upper inset to Fig. 5 shows the inverse of the real part of the dielectric constant after subtraction of the background value of $\varepsilon_\infty = 28$. The data below and above the transition temperature can be well described with a Curie-Weiss law. In addition, no thermal hysteresis was observed between data obtained during cooling and heating. Therefore, as already argued in Ref. 10, these results strongly suggest that the transition is of second order. The transition temperature of $T_c = 97.1$ K agrees with the one published in Ref. 10, but is about 20 K lower than that reported in Ref. 7. A possible origin of this difference may be found in slightly different oxygen concentrations.

The lower inset to Fig. 5 shows the ε'' data measured at frequencies of 3.8 MHz, 346 MHz, 732 MHz, and 1.8 GHz in the temperature region, where a ferroelectric-to-incommensurate phase transition was reported.[9] A small anomaly can be observed at $T \approx 470$ K. However, it is almost unrecognizable in comparison to the transition at $T_c = 97.1$ K.

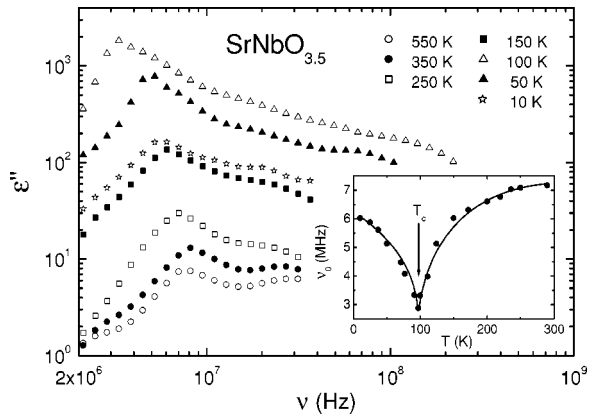

FIG. 6. Frequency dependence of the imaginary part of the complex dielectric constant (ε'') measured at several temperatures in a $SrNbO_{3.5}$ single crystal. The inset shows the temperature dependence of the frequency ν_0, at which ε'' reaches its peak value. The solid line is a guide to the eye.

Figure 6 shows the frequency dependence of ε'' measured at several temperatures in $SrNbO_{3.5}$. Data are shown mainly in the frequency region around 10 MHz, where a peak in ε'' occurs. Usually peaks in $\varepsilon''(\nu)$ arise when the measurement frequency matches the characteristic time, e.g., of a relaxational or resonance process in the sample material. As shown in the inset to Fig. 6, the peak frequency ν_0 exhibits a minimum at the transition temperature $T_c = 97.1$ K. This finding indicates that the observed peak in ε'' is connected to dynamic processes that are closely related to this phase transition. The minimum most probably reflects a slowing down of these processes close to the incommensurate-to-ferroelectric phase transition. However, one has to state that the spectral form of the peak in $\varepsilon''(\nu)$ is untypical for dielectric relaxation or resonance processes, and further investigations of this feature are necessary to understand its nature in full detail.

D. Dielectric properties of $La_{0.2}Sr_{0.8}NbO_{3.5}$ single crystal

In the $La_{0.2}Sr_{0.8}NbO_{3.5}$ sample charge carriers are doped into insulating $SrNbO_{3.5}$ by substituting La^{3+} for Sr^{2+}. Figure 7 shows the frequency dependence of the dielectric constant ε' and conductivity σ' measured at several temperatures in $La_{0.2}Sr_{0.8}NbO_{3.5}$. Solid lines represent fits using the equivalent circuit, presented in Fig. 1. Again, large contact contributions can be observed. Since gold electrodes were used in this case, we can conclude that charge-carrier concentrations leading to different band configurations at the interface is the main reason for this feature. That is, in $SrNbO_{3.5}$ and $SrNbO_{3.45}$ samples with gold electrodes, no contact contributions were observed in the measuring frequency range, while in the $SrNbO_{3.41}$ sample with silver electrodes and the $La_{0.2}Sr_{0.8}NbO_{3.5}$ sample with gold electrodes, distinctive contributions were observed. Indeed, the

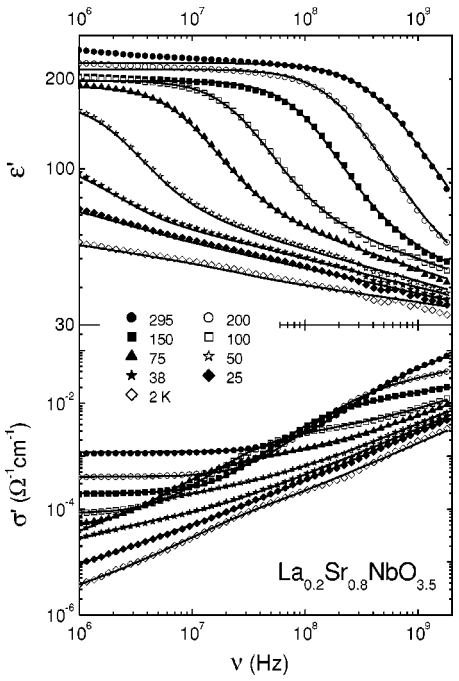

FIG. 7. Frequency dependence of the dielectric constant ε' and conductivity σ' measured at several temperatures in a $La_{0.2}Sr_{0.8}NbO_{3.5}$ single crystal. Solid lines through the experimental data are fits using the equivalent circuit, indicated in Fig. 1.

number of introduced charge carriers in $La_{0.2}Sr_{0.8}NbO_{3.5}$ would correspond to the $SrNbO_{3.40}$ case, thus being much closer to $SrNbO_{3.41}$ than to the other two compounds.

Figure 8 shows the temperature dependence of the fit parameter σ_{dc} and, in the right inset, of the UDR exponent *s*, yielding values for the fit parameters of the small polaron tunneling model of $W_\infty = 3$ meV, $\tau_0 = 1.5\times10^{-17}$ s, and $\alpha r_0 = 140$. Unfortunately, the frequency dependence of ε', as shown in Fig. 7, does not saturate at higher frequencies,

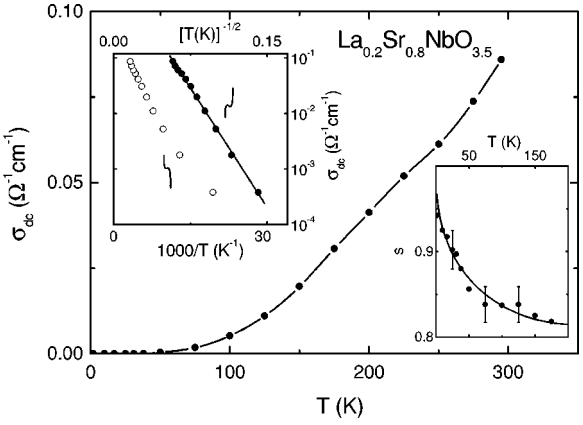

FIG. 8. Temperature dependence of σ_{dc} determined from the fits presented in Fig. 7. The right inset shows the temperature dependence of the UDR exponent *s* with the solid line being a fit with a model for small polaron tunneling. The left inset shows σ_{dc} presented in the Arrhenius representation and in a representation which should linearize the data for VRH with Coulomb interactions (Ref. 25) and one-dimensional VRH (Ref. 24).

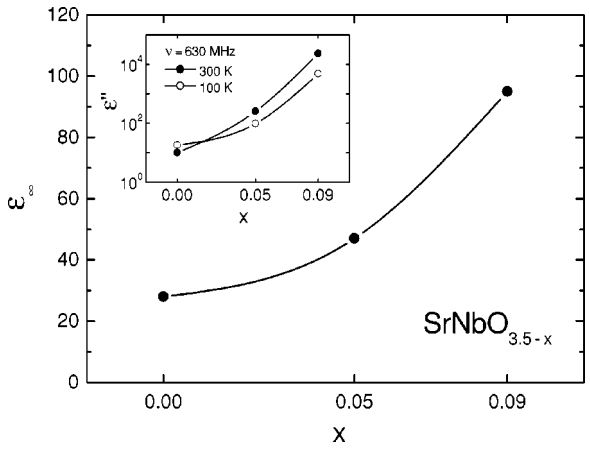

FIG. 9. High-frequency dielectric constant ε_∞ as a function of oxygen content in the $SrNbO_{3.5-x}$ system. The inset shows the imaginary part of the complex dielectric constant, ε'', measured at two different temperatures in all three studied compounds. Solid lines through the data are guides to the eye.

which prevented the determination of ε_∞. Furthermore, at higher temperatures the contact steps in ε' and σ' shift to such high frequencies that even the determination of σ_{dc} is prevented. Therefore, in Fig. 8 we show only results in the temperature region below 300 K. In order to obtain intrinsic data also at higher temperatures, and thus find out if the phase transition, observed in $SrNbO_{3.41}$ and $SrNbO_{3.45}$, also takes place in $La_{0.2}Sr_{0.8}NbO_{3.5}$, further dielectric measurements at frequencies higher than 1.8 GHz are needed.

IV. DISCUSSION

All members of the $SrNbO_{3.5-x}$ family are derived from the layered ferroelectric insulator $SrNbO_{3.5}$. However, by decreasing the oxygen content, more and more charge carriers are doped into this insulating compound. Therefore, the conductivity of the samples increases with decreasing oxygen content, which can be clearly seen by comparing the measured values of σ' in Figs. 1 and 4. Both dc and ac conductivity values are higher in $SrNbO_{3.41}$ than in $SrNbO_{3.45}$. This behavior is also shown in the inset to Fig. 9, where the imaginary part of the complex dielectric constant, ε'', measured at two different temperatures in all three $SrNbO_{3.5-x}$ compounds under investigation, is shown. The values of ε'' increase with decreasing oxygen content. It can also be seen that the dielectric losses decrease with decreasing temperature in both conducting compounds $SrNbO_{3.41}$ and $SrNbO_{3.45}$. In $SrNbO_{3.5}$ the dependence on temperature is different, since this compound undergoes a ferroelectric transition at $T_c \approx 100$ K, where losses reach a peak value.

The main frame of Fig. 9 shows the intrinsic high-frequency dielectric constant ε_∞ in all three $SrNbO_{3.5-x}$ compounds. ε_∞ increases with decreasing oxygen content, i.e., with an increasing number of charge carriers. Since the relatively high values of ε_∞ reflect a high polarizability of the lattice, the formation of polarons seems very possible, especially in the $SrNbO_{3.41}$ system.

In fact, the mechanism governing the electrical transport

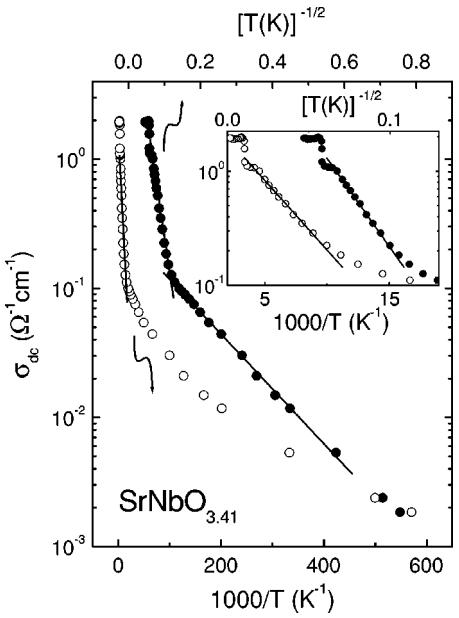

FIG. 10. The dc conductivity data in $SrNbO_{3.41}$, already shown in Fig. 2. Here they are presented in an Arrhenius representation and in a representation which should linearize the data for VRH with Coulomb interactions and one-dimensional VRH. The inset shows an enlarged view of the high-temperature region. The solid line through the open circles is a fit to thermally activated behavior, $\sigma_{dc} \propto \exp(-E_g/2kT)$, which yields $E_g = 20$ meV, while the other solid lines demonstrate VRH behavior.

is one of the most interesting questions concerning semiconducting materials. As already mentioned in Sec. I, based on measurements of the dc conductivity, it was suggested that thermally activated behavior is responsible for the electrical transport in the $SrNbO_{3.41}$ system along the c axis.[2,3,16] In contrast, from the ac conductivity results, presented in Secs. III A, III B, and III D, we conclude that hopping of localized charge carriers (most probably of polaronic nature) plays an important role in the $SrNbO_{3.5-x}$ type compounds. To clarify this discrepancy, the dc conductivity of $SrNbO_{3.41}$, already shown in Fig. 2, is replotted in an Arrhenius representation in Fig. 10 (open circles). The high-temperature region between about 100 and 200 K may indeed follow the thermally activated behavior with an energy gap of about 20 meV (inset). However, the low-temperature results clearly deviate from the Arrhenius behavior, and can be fitted by straight lines in insignificantly small temperature regions only. Alternatively in Fig. 10 a representation is included that should lead to a linearization of the results for a behavior $\sigma_{dc} \sim \exp(T_0/T)^{1/2}$. Such a behavior is typical of variable range hopping (VRH) in one dimension,[24] or alternatively for three-dimensional VRH with strong Coulomb interactions.[25] VRH, involving tunneling of electrons or holes, is the most common model for the description of the dc response of hopping charge carriers. Indeed this representation leads to a linearization of $\sigma_{dc}(T)$ at $T < 80$ K. Therefore, we conclude that hopping of localized charge carriers is also the dominating process for the dc transport in $SrNbO_{3.41}$ at least at low temperatures. As demonstrated in the inset, thermally activated transport and VRH can both describe the experimental data at high temperatures with nearly equal quality. It can be speculated that hopping conduction governs the dc transport in $SrNbO_{3.41}$ at low temperatures only, where band conduction alone would lead to much lower conductivity values. However, considering our finding of UDR at high temperatures, hopping conduction most likely prevails in the complete temperature range investigated. Furthermore, the left inset to Fig. 8 shows the same two representations, mentioned above, of the σ_{dc} data obtained in $La_{0.2}Sr_{0.8}NbO_{3.5}$ in the temperature range of 50–300 K. Again, VRH provides the best description of $\sigma_{dc}(T)$. It can be clearly seen that hopping conduction of localized charge carriers also governs the electrical transport at higher temperatures.

V. CONCLUSIONS

The dielectric responses of insulating $SrNbO_{3.5}$ and quasi-one-dimensional metallic $SrNbO_{3.41}$, $SrNbO_{3.45}$, and $La_{0.2}Sr_{0.8}NbO_{3.5}$ were measured along the c axis in a frequency range from 1 MHz to 1.8 GHz. Due to strong contact contributions to the measured dielectric response, the intrinsic dielectric response in these compounds can be monitored only by performing measurements at high frequencies.

In $SrNbO_{3.5}$ a ferroelectric-to-incommensurate phase transition at $T \approx 473$ K and a second ferroelectric transition at $T_c = 97.1$ K have been detected. Both transitions were already reported in the literature. The transition temperature of $T_c = 97.1$ K agrees reasonably with the one published in Ref. 10, but is about 20 K lower than reported in Ref. 7. In addition, we found evidence of a dynamic process, which significantly slows down close to T_c.

In the conducting compounds $SrNbO_{3.41}$ and $SrNbO_{3.45}$, a phase transition at $T \approx 300$ K has been observed. Due to the relatively high electrical conductivity, which prevented us from performing polarization measurements, it is not possible to deduce if this transition is connected to the above-mentioned transitions in $SrNbO_{3.5}$, i.e., if this is a polar or structural phase transition. Dominating contact contributions at high temperatures prevented the detection of a possible transition in $La_{0.2}Sr_{0.8}NbO_{3.5}$.

The ac conductivity in all three conducting compounds follows the UDR behavior $\sigma'_{ac} \propto \omega^s$, which is also reflected in the real part of the complex dielectric constant; $\varepsilon' \propto \omega^{s-1}$. This indicates a hopping transport of localized charge carriers. The temperature dependence of the exponent s in all three compounds can be well described using a model for small polaron tunneling. The lower value of the hopping barrier in $SrNbO_{3.41}$ than in $SrNbO_{3.45}$, and the increased number of charge carriers, are in accordance with the fact that with lowering the oxygen content in $SrNbO_{3.5-x}$ the conductivity increases. Guided by the very low hopping barriers for $SrNbO_{3.41}$ ($W_\infty = 1.5$ meV) and for the La-doped compound ($W_\infty = 3$ meV), we can conclude that even in our measurements with the ac electric field along the c axis, polarons are very close to delocalization. The intrinsic high-frequency dielectric constant ε_∞ increases with decreasing oxygen content. The relatively high values of ε_∞ determined in the $SrNbO_{3.5-x}$ series, between 30 and 100, reflect a high polar-

izability of the lattice, thus favoring the formation of polarons.

Finally, the dc conductivity data obtained from an equivalent-circuit analysis in $SrNbO_{3.41}$ and $La_{0.2}Sr_{0.8}NbO_{3.5}$ can be well described by assuming a variable range hopping of localized charge carriers. At least at low temperatures the electrical transport along the *c* axis is clearly not thermally activated, as suggested earlier.[2,3,16] Both the results on dc and ac conductivities indicate that the hopping of localized charge carriers governs charge transport along the *c* axis in the $(Sr,La)NbO_{3.5-x}$ system.

ACKNOWLEDGMENTS

This research was supported by the BMBF via VDI/EKM 13N6917 and 13N6918, and partly by the Deutsche Forschungsgemeinschaft via the SFB 484 (Augsburg).

*On leave from Jožef Stefan Institute, Ljubljana, Slovenia.

[1] M. Imada, A. Fujimori, and Y. Tokura, Rev. Mod. Phys. **70**, 1039 (1998).

[2] F. Lichtenberg, T. Williams, A. Reller, D. Widmer, and J.G. Bednorz, Z. Phys. B: Condens. Matter **84**, 369 (1991).

[3] F. Lichtenberg, A. Herrnberger, K. Wiedenmann, and J. Mannhart, Prog. Solid State Chem. **29**, 1 (2001).

[4] N. Yamamoto, Acta Crystallogr., Sect. A: Cryst. Phys., Diffr., Theor. Gen. Crystallogr. **38**, 780 (1982).

[5] S. Kojima, K. Ohi, and T. Nakamura, J. Phys. Soc. Jpn. Suppl. B **49**, 41 (1980).

[6] K. Ohi, Y. Akishige, and M. Hotta, J. Phys. Soc. Jpn. Suppl. B **49**, 98 (1980).

[7] S. Nanamatsu, M. Kimura, and T. Kawamura, J. Phys. Soc. Jpn. **38**, 817 (1975).

[8] N. Isizawa, F. Marumo, T. Kawamura, and M. Kimura, Acta Crystallogr., Sect. B: Struct. Crystallogr. Cryst. Chem. **31**, 1912 (1975).

[9] K. Ohi, M. Kimura, H. Ishida, and H. Kakinuma, J. Phys. Soc. Jpn. **46**, 1387 (1979).

[10] Y. Akishige, M. Kobayashi, K. Ohi, and E. Sawaguchi, J. Phys. Soc. Jpn. **55**, 2270 (1986).

[11] M. Shoyama, A. Tsuzuki, K. Kato, and N. Murayama, Appl. Phys. Lett. **75**, 561 (1999).

[12] J.-E. Weber, C. Kegler, N. Büttgen, H.-A. Krug von Nidda, A. Loidl, and F. Lichtenberg, Phys. Rev. B **64**, 235414 (2001).

[13] C.A. Kuntscher, S. Gerhold, N. Nücker, T.R. Cummins, D.-H. Lu, S. Schuppler, C.S. Gopinath, F. Lichtenberg, J. Mannhart, and K.-P. Bohnen, Phys. Rev. B **61**, 1876 (2000).

[14] C.A. Kuntscher, Ph.D. thesis, University of Karlsruhe (Cuvillier Verlag, Göttingen, 2000).

[15] D.-H. Lu, C.S. Gopinath, M. Schmidt, T.R. Cummins, N. Nücker, S. Schuppler, and F. Lichtenberg, Physica C **282-287**, 995 (1997).

[16] C.A. Kuntscher, S. Schuppler, P. Haas, B. Gorshunov, M. Dressel, M. Grioni, F. Lichtenberg, A. Herrnberger, F. Mayr, and J. Mannhart (unpublished).

[17] R. Böhmer, M. Maglione, P. Lunkenheimer, and A. Loidl, J. Appl. Phys. **65**, 901 (1989).

[18] A.K. Jonscher, *Dielectric Relaxations in Solids* (Chelsea Dielectrics Press, London, 1983).

[19] J. Ross Macdonald, *Impedance Spectroscopy* (Wiley, New York, 1987).

[20] P. Lunkenheimer, M. Resch, A. Loidl, and Y. Hidaka, Phys. Rev. Lett. **69**, 498 (1992); P. Lunkenheimer, G. Knebel, A. Pimenov, G.A. Emelchenko, and A. Loidl, Z. Phys. B: Condens. Matter **99**, 507 (1996); A. Seeger, P. Lunkenheimer, J. Hemberger, A.A. Mukhin, V.Yu. Ivanov, A.M. Balbashov, and A. Loidl, J. Phys.: Condens. Matter **11**, 3273 (1999).

[21] A.R. Long, Adv. Phys. **31**, 553 (1982).

[22] S.R. Elliott, Adv. Phys. **36**, 135 (1987).

[23] M.P.J. van Staveren, H.B. Brom, and L.J. de Jongh, Phys. Rep. **208**, 1 (1991).

[24] N.F. Mott and E.A. Davis, *Electronic Processes in Non-Crystalline Materials* (Clarendon Press, Oxford, 1979).

[25] B.I. Shklovskii and A.L. Efros, *Electronic Properties of Doped Semiconductors* (Springer-Verlag, Berlin, 1984).